Am J Transl Res 2026;18(5):3783-3793
www.ajtr.org /ISSN:1943-8141/AJTR0171833

Original Article

Three-dimensional finite element analysis of bracketless clear aligner expansion with different buccal bone plate thicknesses

Tong Yu[1], Yuhao Yang[2], Yinchang Liu[1], Jie Wu[1], Yi Sun[1], Yi Ouyang[1], Yu Zhang[1], Jiazhi Yu[1], Lu Wang[1], Xiaoguang Li[1]

[1]*Department of Orthodontic, The Affiliated Stomatology Hospital of Jiamusi University, Jiamusi 154000, Heilongjiang, China;* [2]*Department of Oral and Maxillofacial Surgery, The Affiliated Stomatology Hospital of Jiamusi University, Jiamusi 154000, Heilongjiang, China*

Received February 2, 2026; Accepted April 19, 2026; Epub May 15, 2026; Published May 30, 2026

Abstract: Objectives: The thickness of the buccal cortical plate of maxillary posterior teeth limits the safe range of transverse expansion with bracketless clear aligners. Methods: This retrospective study analyzed cone-beam CT data from 100 adults with normal occlusion. Buccal bone plate thickness was measured at four sites (F1-F4: 3, 6, 8 mm apical to cemento-enamel junction and root apex) for maxillary first/second premolars (PM1, PM2) and first/second molars (M1, M2). Based on PM1 thickness at F1 (mean ± SD), three maxillary models with thin (0.42 mm), medium (0.72 mm), and thick (1.02 mm) buccal plates were reconstructed. For each, aligner-dentition-periodontal ligament-bone systems with four buccal root torque angles (0°, 0.5°, 1.0°, 1.5°) were built, yielding 12 finite element models. Periodontal ligament (PDL) stress, tooth displacement, and root control (R/C ratio) of PM1 were analyzed. Results: PM1 exhibited the thinnest buccal plate at F1 (0.72±0.30 mm), significantly thinner than other posterior sites (P<0.001). Thinner plates showed greater crown tipping and higher cervical PDL stress at low torque. Increasing torque to 1.0° promoted bodily movement, reduced peak PDL stress (57.1% reduction in thin-plate model from 0° to 1.0°), and improved root control. Torque of 1.5° showed similar effects. Conclusions: The maxillary first premolar region is highest-risk for buccal dehiscence during clear aligner expansion. Individualizing buccal root torque (≈1.0°-1.5°) based on bone thickness enhances bodily movement, reduces PDL stress, and may improve safety in thin-bone patients.

Keywords: Bracketless clear aligner, clear aligner therapy, maxillary arch expansion, buccal bone plate thickness, torque design, three-dimensional finite element analysis, orthodontic biomechanics

Introduction

Bracketless clear aligners have become a mainstream option for orthodontic treatment in both growing patients and adults, largely because they offer acceptable efficacy with clear advantages in aesthetics and comfort [1, 2]. With the increasing use of clear aligner therapy for transverse correction, clinicians are paying closer attention to its biomechanical impact on the alveolar bone during dental arch expansion. The force system of clear aligner therapy is mainly delivered to the clinical crown, and despite the use of auxiliary designs such as optimised attachments and staged movements, root control in expansion remains relatively limited [3, 4]. As a result, posterior teeth are prone to buccal tipping rather than bodily movement during expansion, which may concentrate stress in the cervical cortical bone and periodontal ligament instead of distributing it along the whole root.

Clinical and cone-beam computed tomography (CBCT)-based investigations have shown that excessive buccal displacement can aggravate alveolar bone dehiscence and fenestration, and that orthodontically induced bone defects may compromise periodontal support and long-term stability [5-7]. Once formed, such defects can be difficult to manage and may necessitate complex restorative, endodontic or periodontal

https://doi.org/10.62347/EYJB3618

intervention, further raising the biological and economic cost of treatment. This underscores the need to evaluate the patient's alveolar bone morphology before expansion and to avoid uncontrolled tooth movement, as even unintended minor displacements - such as those reported around fixed lingual retainers - can lead to unfavourable root positions within the cortical housing [8]. Periodontal phenotype and buccal bone plate thickness have therefore been emphasized as key determinants of safe orthodontic movement, and soft- or hard-tissue augmentation has been advocated in selected thin-bone cases prior to active tooth movement [9].

In the maxillary posterior region, the thickness of the buccal cortical plate shows marked inter-individual and site-specific variation, and the first premolar area is often suspected to present a relatively thin buccal plate. During arch expansion with clear aligners, these anatomical differences are likely to influence the location and magnitude of stress within the periodontal ligament and alveolar bone, as well as the tendency of the tooth toward tipping versus bodily movement. However, most existing biomechanical studies on clear aligners have focused on overall tooth displacement, attachment design or anchorage strategies, and have generally used simplified bone geometries that do not systematically incorporate patient-derived variation in buccal bone plate thickness [10, 11]. At the same time, many imaging studies have been limited to two-dimensional measurements, single tooth positions or the anterior region, making it difficult to extrapolate their conclusions to three-dimensional expansion of the maxillary posterior arch in specific ethnic groups.

CBCT now allows reliable three-dimensional reconstruction of the alveolar housing and precise measurement of buccal bone plate thickness along the root. When these data are integrated into subject-specific finite element models, it becomes possible to simulate different torque prescriptions and expansion strategies under realistic boundary conditions, and to quantify their effects on tooth displacement pattern and stress distribution in the periodontal ligament-bone complex. Finite element analyses of clear aligner mechanics have already highlighted how changes in anchorage and force design alter the force-moment system acting on teeth, reinforcing the importance of carefully calibrated biomechanics in aligner therapy.

Against this background, previous finite element studies of clear aligner mechanics have shown how changes in anchorage and force design alter the force-moment system acting on teeth; however, very few investigations have integrated population-based cone-beam CT measurements of buccal bone plate thickness into subject-specific three-dimensional models of clear aligner expansion. The present study first characterizes the distribution of buccal bone plate thickness in the maxillary posterior region based on CBCT measurements in a Chinese adult population, identifying sites that are particularly susceptible to dehiscence risk during expansion. On this basis, three-dimensional finite element models of a bracketless clear aligner-maxillary dentition-periodontal ligament-alveolar bone system with different buccal bone plate thicknesses and graded buccal root torque are constructed. By analysing tooth displacement patterns, periodontal ligament stress fields and the degree of root control under different torque levels, the study aims to elucidate the interaction between buccal bone plate thickness and torque in root-controlled expansion. The ultimate goal is to provide a biomechanical reference for designing torque prescriptions and expansion strategies that respect the anatomical limits of the buccal bone plate, improve the safety of clear aligner arch expansion, and inform clinical decision-making in patients treated in East and South Asian populations, including India.

Materials and methods

Design

The study consisted of two parts: a retrospective cross-sectional cone-beam CT analysis and a three-dimensional finite element analysis.

Time and place

This experiment was completed between January-July 2025 at the Experimental Centre of Stomatology Engineering, Jiamusi University.

Materials/subjects

Main software and equipment: Cone-beam CT (Sirona, Germany), computer (Alienware, USA), Mimics 21.0 software (Materialise, Leuven, Belgium), Geomagic Wrap 2021 software (3D System, USA), 3-matic 13.0 software (Materialise, Leuven, Belgium), SolidWorks 2021 software (Dassault Systemes, USA), Ansys Workbench 19.0 software (Swanson Analysis, USA).

Subjects: This retrospective study included patients who were screened for reasons such as orthodontic treatment or third molar extraction from January 2024 to January 2025, and who had their maxillofacial CBCT taken at the Affiliated Stomatological Hospital of Jiamusi University. Inclusion criteria: ① Age 20-30 years old; ② Individual normal occlusion or mild malocclusion (without prior orthodontic treatment); ③ Complete dentition (except third molar); ④ Healthy periodontal tissues without serious bone defects. Exclusion criteria: ① History of maxillofacial surgery, trauma or congenital malformation; ② History of orthodontic treatment; ③ Artifacts in the CBCT images, which affected the measurement of key areas. A total of 100 patients (50 males and 50 females), with a mean age of (24.5±2.8) years, were finally included as the case data for measurement and analysis, and a total of 800 teeth (n = 800) were targeted for measurement and analysis in each case, respectively, with the bilateral maxillary first premolar, second premolar, first molar, and second molar [12, 13]. CBCT data of a 26-year-old healthy male volunteer (mild dental crowding with arch narrowing, missing third molar, periodontal health, no significant bilateral temporomandibular joint abnormalities, no history of orthodontic treatment, and no history of systemic diseases) were selected from the measurement sample for modelling. The experimental protocol was approved by the Medical Ethics Committee of the Affiliated Stomatological Hospital of Jiamusi University (Ethical Review No. KQYXY-2025-XX-M037). Written informed consent was obtained from all participants prior to CBCT imaging and the use of their anonymised data for research purposes.

Measurement of buccal lateral bone plate thickness

The imaging data of all the included volunteers were provided by the Department of Radiology of the Affiliated Stomatological Hospital of Jiamusi University, and the data of the bilateral maxillary first premolar (PM1), the second premolar (PM2), the first molar (M1), and the second molar (M2) were respectively 3D reconstructed by using the system's own SIDEXIS XG software version 3.7 analysis software. Three-dimensional reconstruction was performed [14-16]. The 3D reconstruction image cropping frame was adjusted to the teeth to be measured, the image brightness and grey scale values were adjusted to make the indirect image of the tooth and bone tissue clear, the axial plane was adjusted to the maximum periapical diameter of the tooth, and the image was enlarged to the maximum magnification (150% magnification) in the sagittal window to the middle of the tooth to make sure that the sagittal plane passed the convexity of the labial surface, and in the coronal plane the sagittal plane was allowed to pass through the cusp and apices of the tooth, with the axial axis parallel to the long axis of the body, and the image was made to be parallel to the long axis of the body of the tooth [17]. The long axis of image cropping was kept parallel to the long axis of the tooth, i.e., the section could show a clear and complete image of the root and root canal of the tooth (**Figure 1**). The starting point of the measurement was set at the enamel-osseous boundary (CEJ) corresponding to the midline of the buccal surface of the crown of the tooth, which was extended perpendicularly to the long axis of the tooth to the root side by 3 mm, 6 mm, and 8 mm, and the apical point was measured to determine the thickness of the cortex of the bone at that point (**Figure 1**). The four measurement levels were designated as F1 (3 mm), F2 (6 mm), F3 (8 mm), and F4 (root apex). All measurements were performed by the same trained researcher, and repeated 3 times for each tooth position, and the final mean value was recorded with an accuracy of 0.01 mm. To assess intra-examiner reliability, 20 randomly selected CBCT datasets were re-measured after a two-week interval. The intraclass correlation coefficient (ICC) for the repeated measurements was 0.96 (95% confidence interval: 0.94-0.98), indicating excellent measurement consistency. All measurements were entered into a database using Excel software and analysed by SPSS 22.0 software. A two-way analysis of variance (ANOVA) was performed to evaluate the effects of tooth type (PM1, PM2, M1, M2) and measurement site (F1-F4) on buccal bone plate thickness. Pairwise comparisons among different teeth and sites were conducted using Tukey's Honestly Significant Difference (HSD) post-hoc test to adjust for multiple comparisons. A *P*-value <0.05 was considered statistically significant.

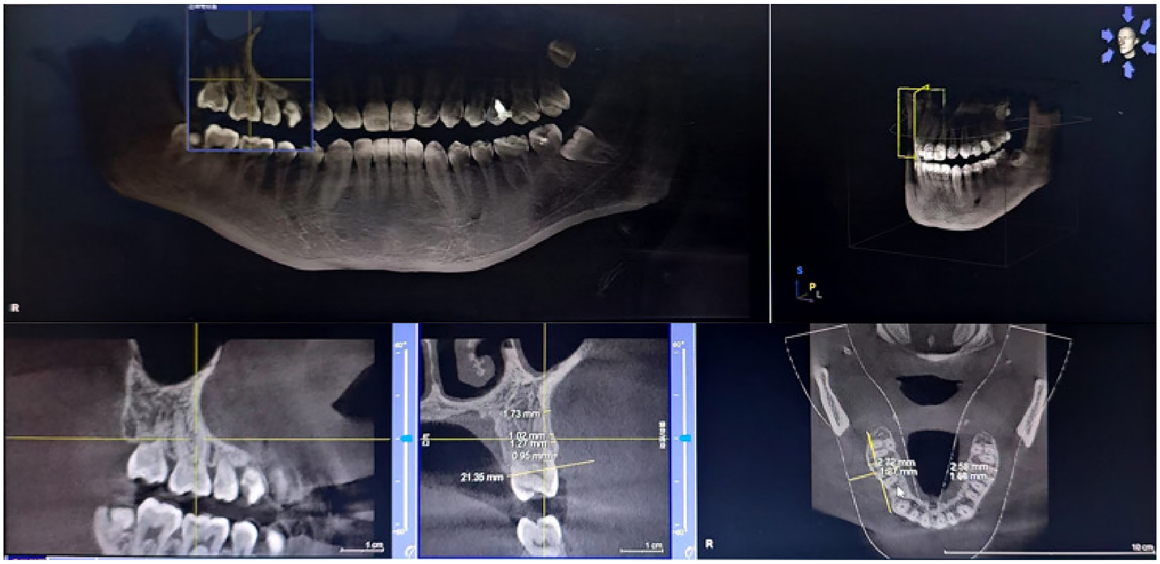

Figure 1. CBCT measurements.

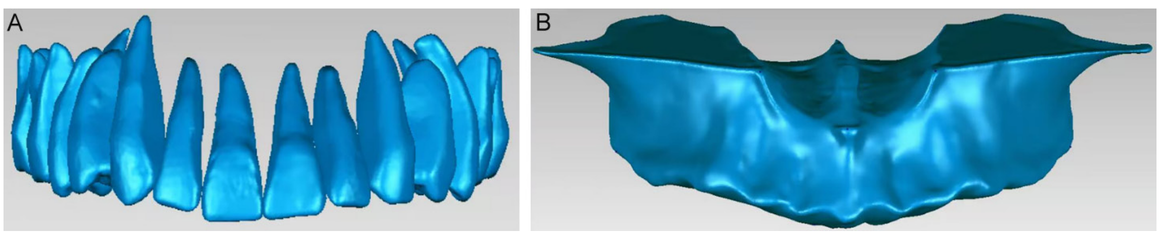

Figure 2. Geomagic Wrap software refinement. A: Maxillary dentition; B: Maxilla.

Three-dimensional finite element model building

Geometric model extraction: Data from the volunteer was obtained from the cone-beam CBCT, stored in DICOM format, imported it into Mimics 21.0 software, 3D orientation was determined, a mask was created by adjusting the grey scale threshold according to the density of each part of the human body's hard tissues, the range of the threshold was adjusted, with segmentation and reconstruction of individual teeth and maxilla, data of the maxillary dentition and the maxilla was extracted, and a maxillary 3D model reconstruction was performed and exported in STL format.

Model optimization and materialization: The STL model was imported into Geomagic Wrap 2021 software, and each 3D model was refined in the polygon toolbar by redrawing the mesh, removing the pegs, relaxing and smoothing, as shown in **Figure 2**, and according to the results of the first part of the measurements, the emphasis was placed on modifying the thickness of the buccal plate in the PM1 region by means of 'Surface Offset', and the thickness of the buccal plate in PM1 region was modified. According to the results of the first part of the measurement, we focused on modifying the thickness of the buccal plate in PM1 area. Through the function of 'Surface Offset', we generated three maxillary models with thin, medium, and thick buccal bone plates for PM1, based on the distribution of thickness at the F1 site (0.72±0.30 mm). These were recorded as Model A (thin: mean - 1 SD = 0.42 mm), Model B (medium: mean = 0.72 mm), and Model C (thick: mean + 1 SD = 1.02 mm), respectively, in **Figure 3.** This approach allows the simulation to cover the clinically relevant spectrum of bone thickness in the population.

Establishment of periodontal membrane and alveolar bone model: In Geomagic Wrap 2021 software, the maxillary tooth model was offset

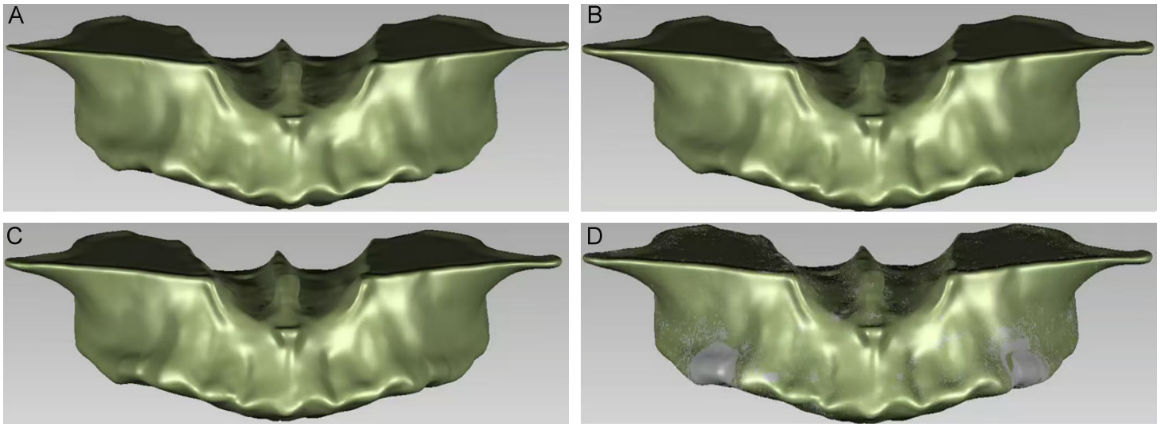

Figure 3. Geomagic Wrap software materialisation of the maxillary dentition and maxilla. Note: A-C: Maxillary models with PM1 cej-3 mm buccal bone plate thicknesses of thin, medium and thick, respectively; D: Overlaid images of three sets of maxillae. PM1, first premolar; CEJ, cemento-enamel junction.

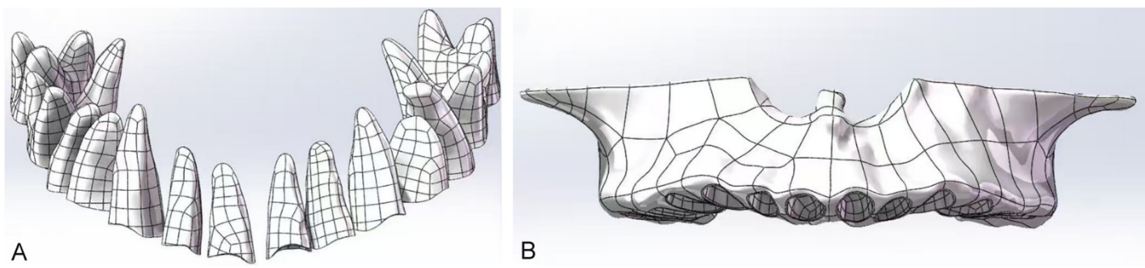

Figure 4. Solidworks software to build periodontium and alveolar bone. A: Periodontium; B: Alveolar bone.

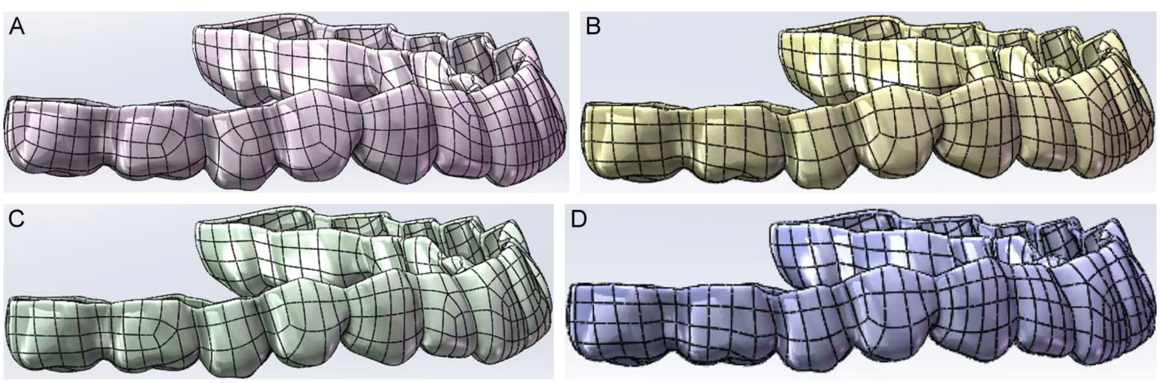

Figure 5. Models of different torque angles of Invisalign. A: 0° torque; B: 0.5° torque; C: 1.0° torque; D: 1.5° torque.

0.25 mm outward as a whole and then solidified to construct the periodontal membrane, which was exported in STEP format in **Figure 4**.

Establishment of the Invisalign model: In Geomagic Wrap 2021 software, the process of arch expansion was simulated: the bilateral maxillary posterior teeth (PM1, PM2, M1, M2) were shifted buccally by 0.2 mm as a whole, and the end positions of the teeth were obtained. On this basis, a root-buccal torque was applied to the crown of PM1 to produce buccal movement of the tooth root, with four sets of torque angles of 0°, 0.5°, 1.0°, and 1.5°, respectively. Based on the shape of the crowns in the final position, four models of 0.75-mm-thick Invisalign aligners were generated by 'surface offset', as shown in **Figure 5**, and the experimental groups are shown in **Table 1**.

Table 1. Experimental grouping

Model Number	Buccal Bone Plate Thickness (mm)	Torque Angle (°)
A1	0.42	0
A2	0.42	0.5
A3	0.42	1
A4	0.42	1.5
B1	0.72	0
B2	0.72	0.5
B3	0.72	1
B4	0.72	1.5
C1	1.02	0
C2	1.02	0.5
C3	1.02	1
C4	1.02	1.5

Table 2. Material properties in 3D finite element model

Material	Elastic Modulus (MPa)	Poisson's Ratio
Tooth	19,600.00	0.30
Periodontal Ligament	0.68	0.45
Cortical Bone	13,700.00	0.30
Cancellous Bone	1,370.00	0.30
Bracketless Invisible Aligner	528.00	0.36

Table 3. Total number of nodes and elements in finite element model

Model number	Total number of nodes	Total number of units
A1	339681	180057
A2	340145	180393
A3	338667	179524
A4	339049	179744
B1	339548	179956
B2	340012	180292
B3	338534	179423
B4	338466	179384
C1	339635	180014
C2	340099	180350
C3	338621	179481
C4	338553	179442

Model assembly and import: The above models of teeth, periodontium, jaws and orthodontic appliances were assembled in SolidWorks 2021 to ensure the correct positional relationship of the components. The assembly was imported into ANSYS Workbench 19.0 software in STEP format.

Establishment of finite element model: The above established models of Invisalign, maxillary dentition, periodontal membrane and maxillary bone wewr Imported into SolidWorks 2021 software for assembly to obtain the three-dimensional finite element model of Invisalign-maxillary dentition-periodontal membrane-alveolar bone, and it was saved in XT format.

Three-dimensional finite element analysis

The finite element model was imported into Ansys Workbench 19.0 software, and the material properties of each part of the model were set, the grid was divided, the boundaries were constrained and the coordinate system was established.

Setting material properties: It is assumed that the Invisalign appliance, teeth, periodontium and alveolar bone are isotropic, continuous and homogeneous linear elastic materials. Based on previous studies, the material properties of each part are shown in **Table 2**.

Grid division: the grid cell size of the maxilla was set to 2 mm, the grid cell size of the teeth and the Invisalign aligners was set to 1 mm, and the grid cell size of the periodontium was set to 0.2 mm. The number of nodes and cells for each group of models is shown in **Table 3**.

Setting boundary conditions: In this study, the boundary constraints of the alveolar bone were set as fixed constraints, the periodontium and the alveolar bone, the periodontium and the teeth were set as bound contacts, the contact surfaces of adjacent teeth were set as non-separated, and the teeth and the Invisalign appliance were set as friction contacts with a friction coefficient of 0.2.

Establishment of the coordinate system: Based on the basic symmetry of the left and right sides of the model, only the right first premolar was analysed and discussed in this study. A common coordinate system was used to establish the maxillary right coordinate system, and the X axis was set as the buccolingual direction, with the lingual side being positive; the Y axis was set as the proximal and distal-

Table 4. Comparison of bone plate thickness at different measurement sites on the labial side of maxillary premolar and molar teeth (mm, n = 800)

Site	PM1		PM2		M1 Proximal mesiobuccal root		M1 Distal mesiobuccal root		M2 Proximal mesiobuccal root		M2 Distal mesiobuccal root	
	$\bar{X}\pm s$	p	$\bar{X}\pm s$	p	$\bar{X}\pm s$	p	$\bar{X}\pm s$	p	$\bar{X}\pm s$	p	$\bar{X}\pm s$	p
F1	0.72±0.30	0.01	1.07±0.46	0.01	0.89±0.42	0.01	1.24±0.52	0.01	1.59±0.66	0.01	1.81±0.63	0.01
F2	0.76±0.41	0.01	1.27±0.60	0.01	0.99±0.52	0.01	1.49±0.60	0.01	2.11±0.78	0.01	2.16±0.79	0.01
F3	0.87±0.40	0.01	1.27±0.68	0.01	1.08±0.65	0.01	1.52±0.68	0.01	2.53±1.09	0.01	2.45±1.02	0.01
F4	1.18±0.56	0.01	2.05±0.84	0.01	2.09±1.00	0.01	2.36±1.12	0.01	3.78±1.31	0.01	3.35±1.54	0.01

Note: Data are shown as mean ± SD. A two-way ANOVA (factors: tooth type and measurement site) followed by Tukey's HSD post-hoc test was used for multiple comparisons. The *P*-value in each cell represents the significance of the comparison between that specific tooth-site thickness and the thickness at the thinnest site (PM1 at F1), adjusted by the Tukey HSD test. P<0.05 indicates a statistically significant difference. F1-F4 are defined in the text. Abbreviations: PM1, first premolar; PM2, second premolar; M1, first molar; M2, second molar; F1-F4, measurement sites 3, 6, 8 mm apical to the cemento-enamel junction and root apex, respectively.

medial direction, with the distal-medial side being positive; and the Z axis was set as the vertical direction, with the root side being positive.

Setting of working conditions: This study was a 3 (bone plate thickness) × 4 (torque angle) two-factor design, with a total of 12 groups of analysed working conditions.

The main observation indexes: The distribution of Von-Mises Stress in the periodontium of the maxillary first premolar (3 mm from the root of the CEJ), the tooth movement pattern, and the ability of each group of appliances to control the buccal movement of the maxillary first premolar (R/C value, i.e., the ratio of the amount of root movement to the amount of crown movement) were extracted and analysed.

Results

Thickness of buccal plates of maxillary posterior teeth at each measurement site

The two-way ANOVA revealed that both tooth type and measurement site significantly influenced buccal bone plate thickness (P<0.001 for both), with a significant interaction between them (P<0.001). Post-hoc comparisons showed that the buccal bone plate at F1 of the maxillary first premolar (0.72±0.30 mm) was significantly thinner than at all other sites and teeth (P<0.05). Furthermore, at each tooth position, the thickness at F1 was significantly less than at the apical F4 site (P<0.05). Detailed pairwise comparisons among all tooth-site combinations are presented in **Table 4**, with *P*-values adjusted by Tukey's HSD test.

Distribution of first premolar periodontal equivalent force in each group model

The periodontal equivalent stresses in the first premolar in the 12 groups of models are shown in **Figure 6**. The maximum periodontal equivalent force of the first premolar appeared at 0.22678 MPa in Case A2, and the high stress area was concentrated in the 3 mm area corresponding to the root of the CEJ in PM1, which was mainly concentrated in the periodontal neck, and the increase of the torque to 1.0°-1.5° could effectively reduce the stress distribution level in this area. When the thickness of the buccal bone plate was different, the equivalent periodontal stresses of the first premolar in Case A3, Case B3 and Case C3 were the smallest in Groups A, B and C, respectively. As the torque increased from 0° to 1.0°, the equivalent force decreased in all models and increased from 1.0° to 1.5°. In model A, the stress value at 1.0° torque condition was 57.1% lower than that at 0°.

Trend analysis of tooth displacement

The ability of the aligner to control tooth movement is represented by the R/C value, which is the ratio of root movement to crown movement. As shown in **Figure 7** buccal tooth movement occurs in all working conditions. The root to crown movement tends to be opposite, so the ratio is negative, and the closer the ratio is to 0, the smaller the relative movement of the root to the crown, and the more effective the appliance is in controlling tooth movement. At 0° (negative control) and 1.5° torque, all teeth showed significant crown buccal tilt movement, and this trend was most pronounced in model A, which had the thinnest bone plate. As the

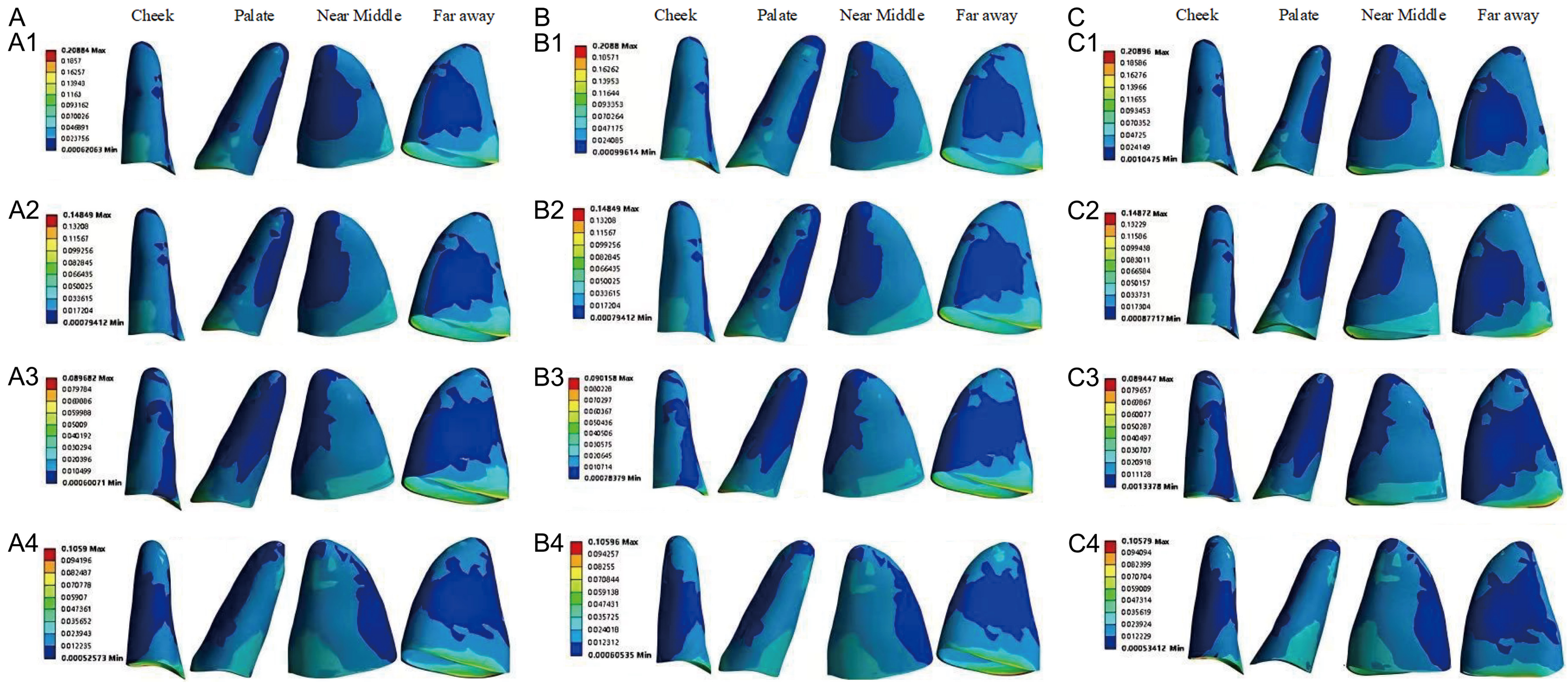

Figure 6. Distribution of PM1 periodontal equivalent force in trayless orthodontic treatment for each working condition. Note: (A-C) in the figure represent the bone models of PM1 with buccal plate thicknesses of 0.42, 0.72, and 1.02 mm, respectively, and 1-4 represent the aligner models of PM1 with root buccal torque angles of 0°, 0.5°, 1.0°, and 1.5°, respectively. PM1, first premolar.

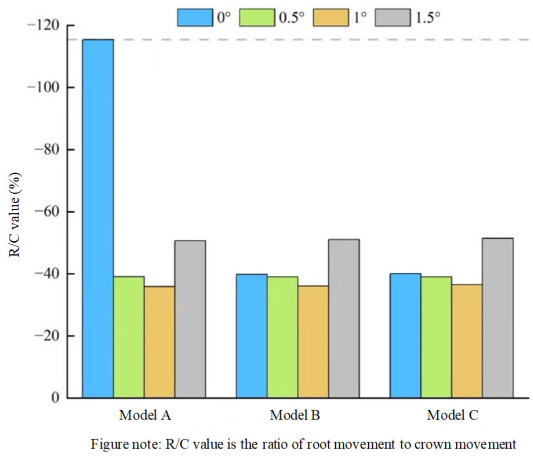

Figure 7. PM1 R/C values in bracketless orthodontic models for each group. PM1, first premolar; R/C, root movement to crown movement ratio.

applied root-buccal torque was increased to 1.0°, the teeth moved in an overall manner.

Discussion

Invisalign arch expansion is a slow arch expansion, which focuses on buccal tilting movement of the teeth as well as alveolar bone remodelling, and is suitable for patients with mild-to-moderate crowding accompanied by dental arch narrowing [18-20]. In this study, we systematically investigated the biomechanical influence of the buccal lateral bone plate thickness, a key anatomical factor, on the effectiveness of arch expansion with the Invisalign trayless appliance using a combination of clinical measurements and biomechanical simulation.

In this study, it was found that the bone tissue in the 3-mm area at the root of the PM1 CEJ was significantly weak, which was the core risk area of bone cracking caused by bow expansion. This area showed significant biomechanical sensitivity in the expansion of invisible bracketless bows as analysed by three-dimensional finite element analysis. The thin bone group showed a significant increase in isometric force when expanding the bow compared with the thick bone group, and the appliance was less capable of controlling the root of the thin bone group. The distribution of equivalent force decreased in all models as the torque increased from 0° to 1.0°, with an increasing trend from 1.0° to 1.5°. In model A, the stress values for the 1.0° torque condition were significantly lower than those at 0°, with a significant increase in root control and an overall trend of tooth movement. Adjusting the root buccal torque angle to 1.0° can effectively reduce the stress value and make the tooth tend to move as a whole.

This study confirms biomechanically that the thickness of the buccal bone plate is a key factor affecting the safety of expanding the arch of Invisalign without brackets. The finding that a moderate buccal root torque of 1.0°-1.5° promotes more bodily movement and reduces PDL stress in thin bone aligns with previous finite element research on anterior teeth [21], which emphasized the crucial role of torque control in facilitating root engagement with the cortical plate. Our study extends these biomechanical principles to the maxillary posterior region during expansion, providing a quantitative reference for torque design in patients with varying buccal bone thickness. However, the model was derived from a single volunteer, which did not cover the variations in jaw morphology. In the future, it is necessary to carry out a large-sample study to establish a database of 'bone thickness-safe arch expansion-ideal torque' for different populations. The three-dimensional finite element analysis used idealised material properties, and the material type also affects the distribution of influence, thus affecting tooth movement, which needs to be further verified by rigorous clinical studies. In addition, no attachments were involved in this study, and exploring the design of a new type of attachments for the Invisalign aligners is also an important direction for future research.

This study has several limitations. First, in line with common practice in FEA studies, all tissues (teeth, PDL, bone, and aligner) were modelled as linear, isotropic, and homogeneous materials. This represents a significant simplification of biological reality, as it does not fully capture the complex biomechanical behaviour of the periodontium and bone. The periodontal ligament is known to exhibit non-linear, viscoelastic behavior under physiological loading, which may influence stress distribution and tooth movement patterns. Second, only the maxillary arch was simulated, without considering mandibular contacts and muscular forces. Third, the finite element results reflect immediate mechanical responses and do not account for biological adaptation or long-term remodelling. Therefore, the present findings should be interpreted as biomechanical guidance, and further clinical and radiographic studies are needed to validate the predicted stress patterns and tooth movements.

Acknowledgements

This study was supported by the Basic Research Funds for Basic Research Projects of the Provincial Department of Education (No. 2023-KYYWF-0615).

Disclosure of conflict of interest

None.

Address correspondence to: Xiaoguang Li, Department of Orthodontic, The Affiliated Stomatology Hospital of Jiamusi University, No. 522 Hongqi Street, Jiaoqu District, Jiamusi 154000, Heilongjiang, China. E-mail: 19354353485@163.com

References

[1] Inchingolo AD, Dipalma G, Ferrara I, Viapiano F, Netti A, Ciocia AM, Mancini A, Malcangi G, Palermo A, Inchingolo AM and Inchingolo F. Clear aligners in the growing patient: a systematic review. Children (Basel) 2024; 11: 385.

[2] Xia Q, Wang W, Wang C, Feng G, Wang C, Song J and Fan Y. Comparative assessment of orthodontic clear aligner versus fixed appliance for anterior retraction: a finite element study. BMC Oral Health 2024; 24: 80.

[3] Bhate M, Jain RK and Balasubramaniam A. Effectiveness of clear aligner therapy in maxillary molar distalization for class II malocclusion: a systematic review of clinical studies. J Int Soc Prev Community Dent 2025; 15: 222-233.

[4] Yangın A, Camcı H and Soybelli M. Clear aligner attachments: a comprehensive review. Turk J Orthod 2025; 38: 177-189.

[5] Sun L, Yuan L, Wang B, Zhang L, Shen G and Fang B. Changes of alveolar bone dehiscence and fenestration after augmented corticotomy-assisted orthodontic treatment: a CBCT evaluation. Prog Orthod 2019; 20: 7.

[6] Song Z, Liu Q, Luo H, Fan X, Zhang M, Liu B, Yan B, Zhang X, Ren L, Ma Y and Jin Z. Factors influencing fenestration and dehiscence in the anterior teeth after clear aligner treatment: a multicenter retrospective study. Prog Orthod 2025; 26: 38.

[7] Rajesh KS, Farooq R, Rajak FA and Kumar P. Treating apical fenestration in a previously endodontically treated tooth. J Conserv Dent Endod 2024; 27: 1193-1195.

[8] Shaughnessy TG, Proffit WR and Samara SA. Inadvertent tooth movement with fixed lingual retainers. Am J Orthod Dentofacial Orthop 2016; 149: 277-286.

[9] Chambrone L and Garcia-Valenzuela FS. Periodontal phenotype modification of complexes periodontal-orthodontic case scenarios: a clinical review on the applications of allogenous dermal matrix as an alternative to subepithelial connective tissue graft. J Esthet Restor Dent 2023; 35: 158-167.

[10] Liu JQ, Zhu GY, Wang YG, Zhang B, Wang SC, Yao K and Zhao ZH. Different biomechanical effects of clear aligners in bimaxillary space closure under two strong anchorages: finite element analysis. Prog Orthod 2022; 23: 41.

[11] Guo R, Lam XY, Zhang L, Li W and Lin Y. Biomechanical analysis of miniscrew-assisted molar distalization with clear aligners: a three-dimensional finite element study. Eur J Orthod 2024; 46: cjad077.

[12] De Clerck HJ and Proffit WR. Growth modification of the face: a current perspective with emphasis on class III treatment. Am J Orthod Dentofacial Orthop 2015; 148: 37-46.

[13] Cevidanes LH, Styner MA and Proffit WR. Image analysis and superimposition of 3-dimensional cone-beam computed tomography models. Am J Orthod Dentofacial Orthop 2006; 129: 611-618.

[14] Frazier-Bowers SA, Simmons D, Wright JT, Proffit WR and Ackerman JL. Primary failure of eruption and PTH1R: the importance of a genetic diagnosis for orthodontic treatment planning. Am J Orthod Dentofacial Orthop 2010; 137: 160, e1-7; discussion 160-1.

[15] Temple KE, Schoolfield J, Noujeim ME, Huynh-Ba G, Lasho DJ and Mealey BL. A cone beam computed tomography (CBCT) study of buccal plate thickness of the maxillary and mandibular posterior dentition. Clin Oral Implants Res 2016; 27: 1072-1078.

[16] Barone S, Paoli A, Razionale AV and Savignano R. Computational design and engineering of polymeric orthodontic aligners. Int J Numer Method Biomed Eng 2017; 33: e2839.

[17] Traversa F, Chavanne P and Mah J. Biomechanics of clear aligner therapy: assessing the influence of tooth position and flat trimline height in translational movements. Orthod Craniofac Res 2025; 28: 1-11.

[18] Ma S and Wang Y. Clinical outcomes of arch expansion with invisalign: a systematic review. BMC Oral Health 2023; 23: 587.

[19] Gonçalves A, Ayache S, Monteiro F, Silva FS and Pinho T. Efficiency of Invisalign First® to promote expansion movement in mixed dentition: a retrospective study and systematic review. Eur J Paediatr Dent 2023; 24: 112-123.

[20] Bouchant M, Saade A and El Helou M. Is maxillary arch expansion with Invisalign® efficient and predictable? A systematic review. Int Orthod 2023; 21: 100750.

[21] Tang XY, Zhang L, Jiang T, Su H, Chen JY, Qin YQ, Fang B and Tang GH. Upper incisal torque movement with clear aligners: a three-dimensional finite element analysis. J World Fed Orthod 2025; 14: 227-234.